Journal of Hazardous Materials 186 (2011) 1398–1404

Contents lists available at ScienceDirect

Journal of Hazardous Materials

journal homepage: www.elsevier.com/locate/jhazmat

Degradation of sulfamonomethoxine with Fe_3O_4 magnetic nanoparticles as heterogeneous activator of persulfate

Jingchun Yan [a], Min Lei [a], Lihua Zhu [a,*], M. Naveed Anjum [a], Jing Zou [b], Heqing Tang [a,*]

[a] College of Chemistry and Chemical Engineering, Huazhong University of Science and Technology, Wuhan 430074, PR China
[b] School of Chemical Engineering and Pharmacy, Wuhan Institute of Technology, Wuhan 430074, PR China

ARTICLE INFO

Article history:
Received 23 April 2010
Received in revised form
15 September 2010
Accepted 6 December 2010
Available online 13 December 2010

Keywords:
Fe_3O_4 magnetic nanoparticles
Persulfate
Sulfate free radical
Sulfamonomethoxine
Degradation

ABSTRACT

Iron oxide magnetic nanoparticles (Fe_3O_4 MNPs) can effectively activate persulfate anions ($S_2O_8^{2-}$) to produce sulfate free radicals ($SO_4^{\bullet-}$), which are a powerful oxidant with promising applications to degrade organic contaminants. The kinetics of sulfamonomethoxine (SMM) degradation was studied in the system of Fe_3O_4 MNPs and $S_2O_8^{2-}$. A complete removal of the added SMM (0.06 mmol L^{-1}) was achieved within 15 min with the addition of 1.20 mmol L^{-1} $S_2O_8^{2-}$ and 2.40 mmol L^{-1} Fe_3O_4 MNPs. There is an optimum concentration of Fe_3O_4 MNPs because Fe_3O_4 MNPs may also act as a $SO_4^{\bullet-}$ scavenger at higher concentrations. It was further observed that the addition of Fe_3O_4 MNPs in several batches for a given total amount of the activator is favorable to enhancing the degradation of SMM. A degradation mechanism was proposed on the basis of identification of the degradation intermediates of SMM with liquid chromatography combined with mass spectroscopy.

1. Introduction

The pollution of PPCPs (Pharmaceuticals and Personal Care Products) in surface and ground water has been an environmental concern in recent years [1–6]. PPCPs are generally resistant to biodegradation. Although their levels in waters may be low, their continuous discharge and low doze exposure in the environment will cause terrible effects in terrestrial and aquatic organisms in long term. Sulfamonomethoxine (SMM, N^1-(6-methoxyl-4-pyrimidinyl) sulfanilamide) is one of the most popular PPCPs normally administered via food, and is widely used for therapeutic or prophylactic proposes for food-producing animal diseases due to its wide spectrum of antibacterial activity and economical advantage [7]. However, its residues generated by unmetabolized excretion or active metabolites being discharged from municipal wastewater treatment plants and agricultural runoff can lead to antibiotic resistant genes, which may be built up and widely transferred among microorganisms. It proves that SMM has a potential impact on environment such as the effects on fertility and thyroid hormone homeostasis in organisms [8]. Therefore, it is important to develop new efficient ways of treating SMM-containing wastewaters.

Advanced oxidation processes (AOPs) have received much attention in recent years due to their potential effectiveness in the degradation and mineralization of organic pollutants [9]. Fenton and Fenton-like processes are one group of the AOPs [10,11]. The Fenton reagent (H_2O_2/Fe^{2+}) has to be used at low pH values (pH < ~3.0) to avoid hydrolysis and precipitation of Fe^{3+}, which is one of the demerits of the Fenton process for the treatment of wastewater. Persulfate ($S_2O_8^{2-}$) is an alternative oxidant, because its activation results in generation of strongly oxidizing sulfate free radicals ($SO_4^{\bullet-}$, $E^0 = 2.6$ V). With the advantages of high solubility, longer residence time in subsurface than peroxide and wide operative pH range [12], persulfate has been successfully used for environmental applications of remediation of trichloroethylene, benzene, toluene, ethylbenzene, xylene, and polychlorinated biphenyls in aqueous and sediment systems [13–16].

$S_2O_8^{2-}$ has to be effectively activated to generate $SO_4^{\bullet-}$ when it is activated by ultraviolet light, heat or transition metal (such as Fe^{2+} and Co^{2+}) [13,14]. Zero-valent iron, supported cobalt catalysts and iron–cobalt mixed oxide were introduced for heterogeneous activation [17–19]. Some of reactions during the activation of $S_2O_8^{2-}$ may be expressed as follows:

$$S_2O_8^{2-} + 2e^- \rightarrow 2SO_4^{2-} \quad E^0 = 2.01\,V \tag{1}$$

$$S_2O_8^{2-} \xrightarrow{\text{heat or UV}} 2SO_4^{\bullet-} \tag{2}$$

$$S_2O_8^{2-} + Me^{n+} \rightarrow Me^{(n+1)+} + SO_4^{\bullet-} + SO_4^{2-} \tag{3}$$

* Corresponding authors. Tel.: +86 27 87543432; fax: +86 27 87543632.
E-mail addresses: lhzhu63@yahoo.com.cn (L. Zhu), hqtang62@yahoo.com.cn (H. Tang).

0304-3894/$ – see front matter © 2010 Elsevier B.V. All rights reserved.
doi:10.1016/j.jhazmat.2010.12.017

$$SO_4^{\bullet -} + e^- \rightarrow SO_4^{2-} \quad E^0 = 2.6\,V \qquad (4)$$

Here, Me represents Fe^{2+} or Co^{2+}. It should be noted that the initiation by UV irradiation is unfavorable to the treatment of UV-absorbing contaminants due to the light filtering effect [20,21]. The activation way of heating consumes a great amount of heat energy. The use of Fe^{2+} for activating persulfate is limited in a narrow pH range. Excess Fe^{2+} ions can also react with $SO_4^{\bullet -}$, independent of the presence of organic substrates, which results in a low efficiency for the utilization of persulfate. The above problems may be partly resolved by using chelating agent such as citric acid and EDTA because the use of chelating agent controls the formation rate of $SO_4^{\bullet -}$ [14].

Fe_3O_4 magnetic nanoparticles (Fe_3O_4 MNPs) have been used as peroxidase mimetic instead of Fe^{2+} to activate H_2O_2 for the removal of organic pollutants [22–24]. Because H_2O_2 and $S_2O_8^{2-}$ are similar in structure of having O–O bond, we anticipate that Fe_3O_4 MNPs are a good candidate for activation of $S_2O_8^{2-}$. The present work aimed at providing insight into the activating ability of Fe_3O_4 MNPs to enhance the decomposition of $S_2O_8^{2-}$ and then degrade organic pollutants: not only an efficient oxidation process was developed to degrade SMM, but also the activation mechanism of persulfate and the degradation mechanism of SMM were clarified.

2. Experimental

2.1. Materials

SMM with a purity of higher than 99% was purchased from Acros (Geel, Belgium). Ferrous sulfate ($FeSO_4{\cdot}7H_2O$), ferric chloride ($FeCl_3{\cdot}6H_2O$), persulfates and ammonia water were obtained from Sinopharm Chemical Reagents (Shanghai, China). All the chemical reagents were of analytical grade and used as received. All solutions were prepared with deionized water. The pH of solution was adjusted with 0.1 mol L^{-1} H_2SO_4 or NaOH.

2.2. Preparation of Fe_3O_4 MNPs

Fe_3O_4 MNPs were synthesized by a modified reverse co-precipitation process without using any dispersant [25]. Solutions of $FeCl_3$ (1 mol L^{-1}, 10 mL) and $FeSO_4$ (1 mol L^{-1}, 10 mL) were mixed well and then heated to 60 °C. The warm Fe^{2+}/Fe^{3+} solution was added dropwise into 45 mL of 3.0 mol L^{-1} ammonia solution located in a ultrasound clean bath operating at 25 kHz with a power of 140 W (KQ-200KDE, China) at 60 °C. After 30 min for the reaction, the solution cooled to room temperature, and the generated Fe_3O_4 MNPs were collected by magnetic separation, washed with water to neutral pH, re-dispersed into 50 mL water and stored for use. The concentration of the Fe_3O_4 MNPs dispersion was determined prior to the experiment.

2.3. Characterization of Fe_3O_4 MNPs

X-ray diffraction (XRD) patterns of dried Fe_3O_4 MNPs were recorded on an X'Pert PRO X-ray diffractometer (PANalytical) with a Cu Kα radiation source generated at 40 kV and 30 mA. The morphology of Fe_3O_4 MNPs was observed with transmission electron microscope (TEM, Tecnai G2 20, Holland) operated at an acceleration voltage of 15 kV. The magnetic properties were performed using ADE 4HF vibrating sample magnetometer at 300 K.

2.4. Degradation experiments

The SMM degradation was carried out in 100 mL conical flask under mechanical stirring at room temperature (25 ± 1 °C) at inherent pH of 6.4 unless specified elsewhere. Typically, Fe_3O_4 MNPs were added into 50 mL of SMM solution (0.06 mmol L^{-1}) and stirred for 20 min to achieve adsorption–desorption equilibrium. Then the concentration of SMM was measured as the initial concentration (c_0). The reaction was initiated immediately by adding persulfate. At regular time intervals, a small volume of the solution (2.0 mL) was sampled and then analyzed after Fe_3O_4 MNPs were removed away by filtering through 0.22 μm membrane. The concentrations of SMM and intermediates were measured with high-performance liquid chromatography (HPLC) and liquid chromatography–mass spectroscopy (LC–MS). Each degradation test was run in triplicate, and the averaged experimental values were then used.

2.5. Analytical methods

The HPLC system consisted of Jasco PU-2089 quaternary gradient pumps with Jasco UV-2075 Intelligent and UV/vis detector (Jasco, Japan). The column was a reversed-phase Spherisorb C_8 column (250 mm × 4.6 mm i.d., 5 μm, Waters). The mobile phase was methanol–water (35:65, v/v) with a flow-rate of 1.00 mL min^{-1} and the effluent was monitored at 265 nm. The mass spectrometer (Agilent 1100 LC/MSD Trap, USA) was operated in electrospray positive ion (ESI^+) mode. The amount of total iron (Fe^{2+} + Fe^{3+}) leached from the Fe_3O_4 MNPs into reaction solutions was monitored by atomic absorption spectroscopy (AAS, Analyst 300, P.E. Inc.), and persulfate was determined with an iodometric method on a Cary 50 UV–vis spectrophotometer (Varian, USA) [26].

3. Results and discussion

3.1. Characterizations of Fe_3O_4 MNPs

XRD patterns of as-prepared Fe_3O_4 MNPs are shown in Fig. 1a. The peaks at 2θ values of 30.1, 35.4, 43.1, 53.6, 57.1 and 62.7° can be indexed as the diffractions of (2 2 0), (3 1 1), (4 0 0), (4 2 2), (5 1 1) and (4 4 0), respectively, which are almost the same as the previously reported data for Fe_3O_4 nanoparticles (JCPDS 79-0419) [27]. On the basis of XRD patterns, the average size of the particles can be evaluated with the Debye–Sherrer formula $D = K\lambda/(\beta \cos\theta)$, where K is the Sherrer constant (0.89), λ is the X-ray wavelength (0.15418 nm), β is the peak full width at half maximum and θ is the Bragg diffraction angle. From the most intense peak (3 1 1), the average size of the particles was calculated to be 17.1 nm.

Fig. 1b gives the TEM image of the Fe_3O_4 MNPs. It indicates that the nanoparticles are spherical with diameters of about 15 nm, which is well in agreement with the value obtained from the XRD results. The saturation moment per unit mass (Ms) for the Fe_3O_4 MNPs was measured to be 68.8 emu g^{-1}. After the activation of $S_2O_8^{2-}$ in the presence and absence of SMM, the Ms value of the used Fe_3O_4 MNPs was 52.9 and 56.1 emu g^{-1}, respectively (SI Fig. S1).

3.2. Establishment of a new activation system for SMM degradation

The influence of different persulfates such as $(NH_4)_2S_2O_8$, $K_2S_2O_8$ and $Na_2S_2O_8$ was checked at first on the degradation of SMM and no noticeable differences were observed between these persulfate, we selected $K_2S_2O_8$ for further researches.

Before extensive studies on the degradation of SMM with persulfate activated by Fe_3O_4 MNPs, we investigated the SMM degradation by using persulfate, Fe_3O_4 MNPs, or leaching solution of Fe_3O_4 MNPs alone in control experiments. When only $S_2O_8^{2-}$ or Fe_3O_4 MNPs were added, the SMM removal was 2.3% and 0.7%, respectively, both of which were ignorable in comparison with almost complete removal of SMM in the presence of

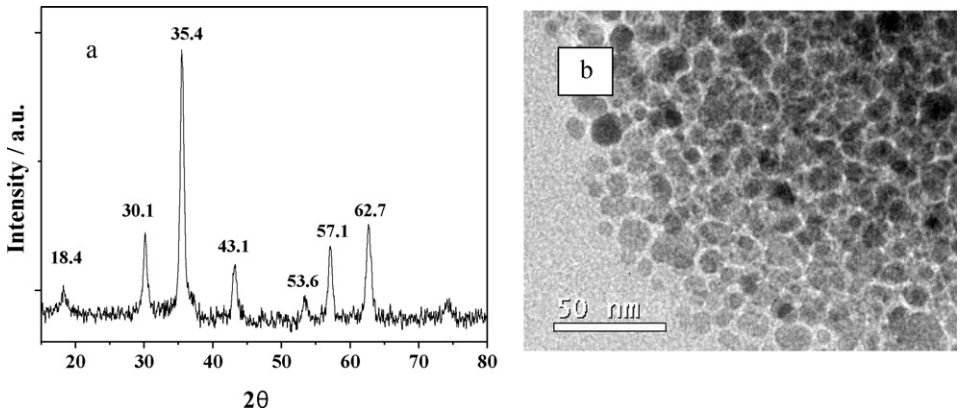

Fig. 1. XRD patterns (a) and TEM image (b) of Fe_3O_4 MNPs prepared by modified reverse co-precipitation method.

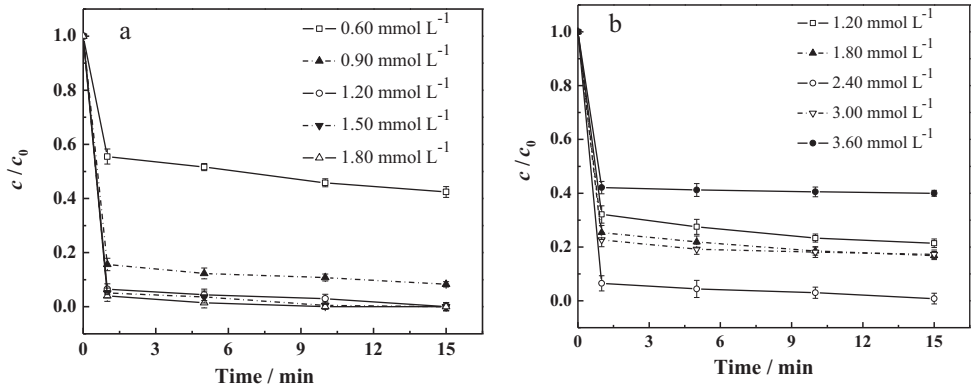

Fig. 2. Kinetic data of the degradation of SMM (c_0 = 0.06 mmol L^{-1}) in the system of $K_2S_2O_8$ and Fe_3O_4 MNPs at pH 6.4: (a) the initial concentration of $K_2S_2O_8$ was varied in the presence of Fe_3O_4 MNPs (2.40 mmol L^{-1}), and (b) the initial concentration of Fe_3O_4 MNPs was varied in the presence of $K_2S_2O_8$ (1.20 mmol L^{-1}).

both $S_2O_8^{2-}$ and Fe_3O_4 MNPs. The significant degradation of SMM in the system of $Fe_3O_4/S_2O_8^{2-}$ may arise from the activation of $S_2O_8^{2-}$ by Fe^{2+} dissolved from Fe_3O_4 MNPs, and we had found 0.03 mmol L^{-1} of total iron ($Fe^{2+} + Fe^{3+}$) in solution after the Fe_3O_4 MNPs (2.40 mmol L^{-1}) were immersed in the test solution in the absence of $S_2O_8^{2-}$ for 3 days. Thus, we also used the leaching solution to activate $S_2O_8^{2-}$. However, the leached Fe^{2+} ions were too little to activate considerable $S_2O_8^{2-}$, corresponding to SMM removal of only 5.9%.

Fig. 2 shows the effects of the concentrations of $S_2O_8^{2-}$ and Fe_3O_4 MNPs on the degradation of SMM at pH 6.4 at 25 °C. The degradation of SMM under all the tested conditions goes very fast at the early stage (t < 1 min) and then very slow at the second stage (t > 1 min). Because all the possible degradation of SMM is almost completed within 1 min, we may use the average rate of SMM degradation over the period from 0 to 1 min, being equivalent to the degradation removal of SMM ($1 - c/c_0$), to evaluate the dependence of SMM degradation on any parameters.

As shown in Fig. 3 (curve 1), the SMM removal within 1 min is increased from 0.7% to 44.5% and then to 96.0% as the concentration of $S_2O_8^{2-}$ is increased from 0 to 0.6 and to 1.8 mmol L^{-1} with the addition of 2.40 mmol L^{-1} Fe_3O_4 MNPs. $S_2O_8^{2-}$ is the origin of driving force for the degradation of SMM. It is reasonable that higher $S_2O_8^{2-}$ concentrations lead to more degradation of SMM. However, $S_2O_8^{2-}$ is activated by Fe_3O_4 MNPs, and hence the influence of $S_2O_8^{2-}$ concentration will become less when the $S_2O_8^{2-}$ concentration is high enough for a given concentration of Fe_3O_4 MNPs. Therefore, it is observed that the increasing of SMM removal is little when $S_2O_8^{2-}$ concentration is higher than 1.2 mmol L^{-1}, which corresponds to $S_2O_8^{2-}$:Fe_3O_4 molar ratio of 1:2.

As an activator, Fe_3O_4 MNPs activate persulfate, yield $SO_4^{\bullet-}$ species, and then accelerate the decomposition of SMM. Therefore, increasing the dose of Fe_3O_4 MNPs is favorable to promoting the degradation of SMM. However, it is found that as the concentration of Fe_3O_4 MNPs is increased from 0 to 2.40 mmol L^{-1}, the SMM removal is increased very fast initially, then increased slowly, and finally decreased (curve 2 in Fig. 3). This observation is closely related to the role of Fe_3O_4 MNPs, which activate the formation of $SO_4^{\bullet-}$ from the decomposition of $S_2O_8^{2-}$, but not for the degradation of SMM. When only a small amount of Fe_3O_4 MNPs is added, a

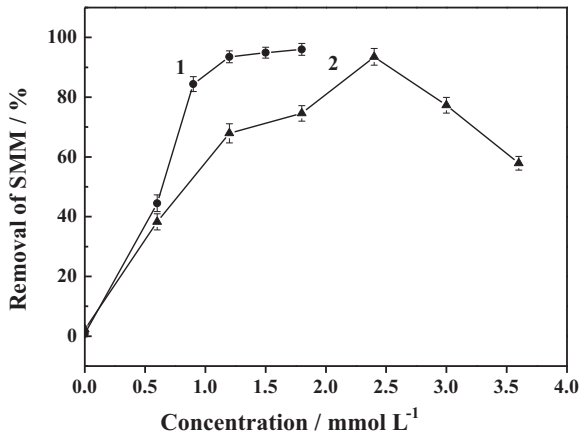

Fig. 3. Effects of the concentrations of (1) $K_2S_2O_8$ and (2) Fe_3O_4 MNPs on the early-stage removal of SMM. The detailed experimental conditions were given in Fig. 2.

considerable amount of $SO_4^{\bullet-}$ is produced, which reacts immediately with SMM, leading to a fast increase of the SMM removal. This is corresponding to the first stage when the concentration of Fe_3O_4 MNPs is less than 1.20 mmol L^{-1}. When Fe_3O_4 MNPs are added in excess, an excess of $SO_4^{\bullet-}$ species are generated, resulting in considerable disappearance of $SO_4^{\bullet-}$ species without the decomposition of SMM due to the combination between $SO_4^{\bullet-}$ species themselves. Moreover, the interaction between excess Fe^{2+} on the surface of Fe_3O_4 MNPs and $SO_4^{\bullet-}$ may directly quench $SO_4^{\bullet-}$ through Eq. (5) [28]:

$$SO_4^{\bullet-} + Fe^{2+} \rightarrow Fe^{3+} + SO_4^{2-} \quad k = 4.6 \times 10^9 \text{ mol L}^{-1} \text{ s}^{-1} \qquad (5)$$

Hence, the SMM removal is decreased when the Fe_3O_4 MNPs are added further beyond about 2.40 mmol L^{-1}. When a moderate amount of Fe_3O_4 MNPs is added, there is a competition between the above-mentioned two effects ($SO_4^{\bullet-}$ quenching and reacting with SMM), which cause slower increasing of the SMM removal with the increase of Fe_3O_4 MNPs addition. This is reflected by the second stage in curve 2 of Fig. 3 (from 1.20 to 2.40 mmol L^{-1}).

The degradation of SMM does not proceed further apparently when the contact time is longer than 1 min, which indicates the decomposition of $S_2O_8^{2-}$ by Fe_3O_4 MNPs is a fast reaction, and an enough amount of $SO_4^{\bullet-}$ is generated transiently once the nanoparticles are attached with $S_2O_8^{2-}$. The apparently quenched degradation of SMM is related to multiple reasons. Firstly, we may consider that all the added persulfate ions have been decomposed completely within 1 min after the nanoparticles are added. However, a residual of about 62.0% of the added $S_2O_8^{2-}$ was found in the system of $S_2O_8^{2-}$/Fe_3O_4/SMM with molar ratio of 20/40/1, suggesting that the complete consumption of the oxidant is not the reason for the much slow degradation of SMM beyond 1 min. Secondly, it is considered that the surface of the nanoparticles is passivated. In order to check it, all the nanoparticles were separated from the above-mentioned solution after a contact time of 15 min and then added into a fresh solution of SMM in the presence of $S_2O_8^{2-}$. We found that the SMM removal was decreased from 100% for the first cycle to 36.9% for the second cycle of using the activator. It is certain that the inactivation of Fe_3O_4 MNPs after contacting the oxidant can partly account for the little degradation of SMM beyond 1 min. Thirdly, we should further consider that the quenching of $SO_4^{\bullet-}$ becomes marked when both the concentrations of the oxidant and SMM are reduced after 1 min for the reaction. Besides, the interaction between Fe^{2+} and $SO_4^{\bullet-}$ may directly quench $SO_4^{\bullet-}$ radicals according to Eq. (5).

Fe_3O_4 MNPs were divided into three equal parts, and added one part into the SMM solution in the presence of persulfate at time intervals longer than 1 min. In this way, both the inactivation of the activator and the quenching of $SO_4^{\bullet-}$ are controlled, and the removal of SMM (46.9%) is considerably higher than that (36.5%) by adding all the catalyst in one time, as shown in Fig. 4. Therefore, the addition of Fe_3O_4 MNPs in several times is favorable to enhancing the degradation efficiency of SMM.

The effect of initial solution pH is investigated on the SMM degradation in the system of 0.06 mmol L^{-1} SMM + 1.20 mmol L^{-1} $S_2O_8^{2-}$ + 2.40 mmol L^{-1} Fe_3O_4 MNPs. It is noted from Table 1 that the SMM degradation is highly efficient in all the tested pH range: the SMM removal achieves 100% at pH < 7.0, and is as high as 78.3% even at pH 10.0. This is a great advantage of the system for wastewater treatment, because it is unnecessary to pre-adjust solution pH.

3.3. Activation mechanism of persulfate on Fe_3O_4 MNPs

Both $SO_4^{\bullet-}$ and $^{\bullet}OH$ were reported to be possibly responsible for the destruction of organic contaminants depending on pH value when $S_2O_8^{2-}$ is activated thermally at ambient temperatures [12]. Recently, we used Fe_3O_4 MNPs to activate H_2O_2 and found that both $^{\bullet}OH$ and $O_2^{\bullet-}$ free radicals are possibly produced from the decomposition of H_2O_2 [23,24]. In order to check the generation of free radicals from the decomposition of $S_2O_8^{2-}$, we used alcohols as the probe. Alcohols with and without R-hydrogen have different reactivity and rate constants in their reactions with radical species. Ethanol (EtOH, containing R-hydrogen) reacts with $^{\bullet}OH$ or $SO_4^{\bullet-}$ at high and comparable rates, and the rate constants for the reaction with $^{\bullet}OH$ and $SO_4^{\bullet-}$ are $(1.2–2.8) \times 10^9$ mol L^{-1} s^{-1} and $(1.6–7.7) \times 10^7$ mol L^{-1} s^{-1}, respectively. However, tert-butyl alcohol (TBA, without R-hydrogen) has much different reaction rate constants, and the rate constant for $^{\bullet}OH$ ($(3.8–7.6) \times 10^8$ mol L^{-1} s^{-1}) is 418–1900 times greater than that for $SO_4^{\bullet-}$ ($(4–9.1) \times 10^5$ mol L^{-1} s^{-1}) [29]. Therefore, the addition of the two alcohols into the oxidation system will change the degradation rate of SMM, and we can clarify what is the dominant free radical generated from the decomposition of $S_2O_8^{2-}$. The test was carried out in the system of 0.06 mmol L^{-1} SMM + 1.80 mmol L^{-1} $S_2O_8^{2-}$ + 3.60 mmol L^{-1} Fe_3O_4 MNPs to ensure all the SMM was completely removed after 15 min without any alcohols addition. It is seen from Table 2 that the addition of 3 mmol L^{-1} TBA (molar ratio TBA/SMM = 50) decreases the SMM removal by about 20% and the addition of 3 mmol L^{-1} ethanol (molar ratio EtOH/SMM = 50) decreases it by about 58% at pH values from 3.0 to 7.0. In presence of the same amount of TBA, a relatively small drop was observed in the degradation removal in comparison with ethanol, indicating that $SO_4^{\bullet-}$ was predominantly produced over $^{\bullet}OH$ during the activated decomposition of $K_2S_2O_8$ by Fe_3O_4 MNPs at pH values from 3.0 to 7.0. At pH values of 8.5 and 10.0, the addition of TBA decreased the SMM removal by 35.9% and that of ethanol decreased by about 58%. Greater decrease was observed at pH 8.5 and 10.0 than that at pH values from 3.0 to 6.8 with the

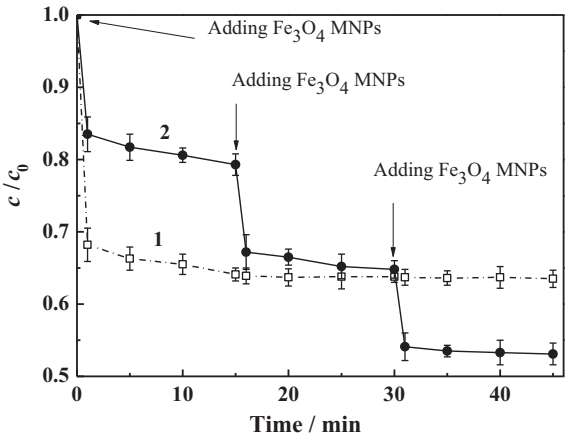

Fig. 4. Influence of the way of adding Fe_3O_4 MNPs on the degradation of SMM: (1) all the Fe_3O_4 MNPs were added in one time, and (2) the Fe_3O_4 MNPs were added in three times after the nanoparticles were divided into three equal portions. Other experimental conditions: c_0 of SMM 0.16 mmol L^{-1}, total amount of Fe_3O_4 MNPs 2.40 mmol L^{-1}, initial concentration of $K_2S_2O_8$ 1.20 mmol L^{-1}, pH 6.4.

Table 1
Effect of initial pH on the degradation of SMM (c_0 = 0.06 mmol L^{-1}) in the presence of Fe_3O_4 MNPs (2.40 mmol L^{-1}) and $K_2S_2O_8$ (1.20 mmol L^{-1}) at 25 °C within 15 min.

Initial pH	Final pH	SMM removal	Consumption of $S_2O_8^{2-}$
3.0	2.6	100%	58.2%
5.5	2.9	100%	56.0%
7.0	3.1	100%	53.2%
8.5	4.3	83.2%	48.7%
10.0	6.9	78.3%	44.3%

Table 2
Effect of ethanol and TBA on the degradation of SMM (c_0 = 0.06 mmol L^{-1}) in the presence of Fe_3O_4 MNPs (3.60 mmol L^{-1}) and $K_2S_2O_8$ (1.80 mmol L^{-1}) at different initial pH values at 25 °C within 15 min.

Initial pH	SMM removal (%)				Major radical species
	Blank[a]	3 mmol L^{-1} EtOH	3 mmol L^{-1} TBA	30 mmol L^{-1} EtOH	
3.0	100	43.1	80.2	11.7	$SO_4^{\bullet-}$
5.5	100	42.0	78.5	11.3	$SO_4^{\bullet-}$
6.8	100	41.6	79.7	12.4	$SO_4^{\bullet-}$
8.5	100	42.8	63.8	11.6	$SO_4^{\bullet-}$/•OH
10.0	100	41.9	64.1	10.9	$SO_4^{\bullet-}$/•OH

[a]Means no addition of any alcohols.

addition of 3 mmol L^{-1} TBA. This suggested that more •OH produced when pH increased to alkaline range in accordance with Eq. (6) [12]:

$$SO_4^{\bullet-} + OH^- \rightarrow SO_4^{2-} + {}^{\bullet}OH \quad k = (6.5 \pm 1.0) \times 10^7 \text{ mol } L^{-1} \qquad (6)$$

The generated •OH reacts with TBA, leading to much decreased removal of SMM. This demonstrates the presence of both $SO_4^{\bullet-}$ and •OH at pH 8.5 and pH 10.0. Both $SO_4^{\bullet-}$ and •OH can react with ethanol with great and similar rate constants, and hence the ethanol-induced decrease in the SMM removal is almost the same at all the tested pH values.

3.4. Mechanism of SMM degradation in the system of persulfate and Fe_3O_4 MNPs

When $SO_4^{\bullet-}$ and •OH attack organic compounds, •OH is more likely to do through hydrogen abstraction or addition reactions, while $SO_4^{\bullet-}$ participates in electron transfer reaction [30]. Thus, different intermediates may be obtained when $SO_4^{\bullet-}$ and •OH react with SMM. In order to check it, SMM was degraded in the systems of $Fe_3O_4/S_2O_8^{2-}$ and Fe_3O_4/H_2O_2 at pH 3.0, respectively, and then the intermediates were analyzed with HPLC. As shown in Fig. 5, the two chromatograms from the two oxidation systems are almost the same as each other in the retention time of the degradation intermediates. This, along with LC–MS identification, suggests that both $SO_4^{\bullet-}$ and •OH result in same degradation intermediates, which can be explained by the following reactions (Eqs. (7)–(10)):

$$SMM + SO_4^{\bullet-} \rightarrow SMM^{\bullet+} + SO_4^{2-} \qquad (7)$$

$$SMM^{\bullet+} + H_2O \rightarrow (OH)SMM + H^+ \qquad (8)$$

$$SMM + {}^{\bullet}OH \rightarrow (OH)SMM \qquad (9)$$

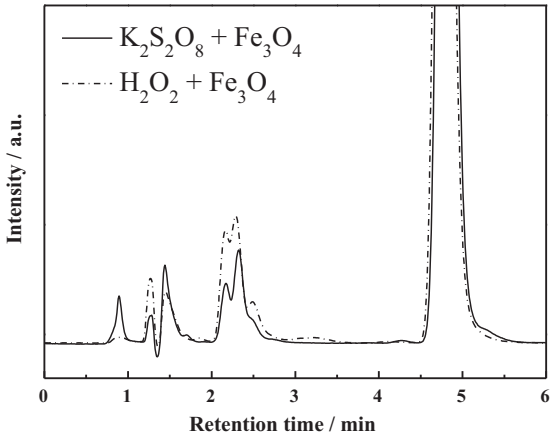

Fig. 5. HPLC diagrams of the solutions of SMM (c_0 = 0.06 mmol L^{-1}) after a degradation time of (1) 10 min in the presence of 0.60 mmol L^{-1} $K_2S_2O_8$ and 1.20 mmol L^{-1} Fe_3O_4 MNPs and (2) 30 min in the presence of 0.60 mmol L^{-1} H_2O_2 and 0.43 mmol L^{-1} Fe_3O_4 MNPs at pH 3.0.

$$(OH)SMM \rightarrow \text{intermediates} \rightarrow CO_2 + H_2O \qquad (10)$$

When $SO_4^{\bullet-}$ participates the reaction, electron-transfer process occurs to form SMM radical cation ($SMM^{\bullet+}$), which reacts quickly with H_2O by way of hydroxyl abstraction or addition reaction to generate (hydroxyl) SMM radicals ((OH)SMM). While •OH attacks SMM molecule, (OH)SMM is preferentially generated through hydrogen abstraction or addition reaction. Therefore, same major intermediates are produced in the systems of $Fe_3O_4/S_2O_8^{2-}$ and Fe_3O_4/H_2O_2 at pH 3.0.

It has been reported that sulfonamide is susceptible to be degraded by singlet oxygen ($^1O_2$) and hydroxyl radical generated by UV irradiation, ozone, photocatalysis using TiO_2 and Fenton reagent [31]. Boreen et al. [32,33] reported that sulfur dioxide extrusion product was the major product during photolysis of sulfonamides containing five- or six-membered heterocyclic substituents. Both organic micromolecules and inorganic products, such as sulfate, nitrate and ammonium ions occurred through the cleavage of the S–N bond and the opening of the thiazole ring during the photocatalysis process of sulfonamides on TiO_2 [34,35]. To better understand the degradation mechanism of SMM in the $Fe_3O_4/S_2O_8^{2-}$ system, the by-products of SMM were identified with LC–MS. The intermediates detected in LC–MS according to retention times (t_R) of peaks and the total ion chromatogram of identified substances are shown in Fig. 6.

The MS spectra of SMM (SI Fig. S2) showed a protonated molecular ion peak at m/z 281 with retention time of 3.6 min. It is attributed to the parent compound of SMM in accordance with the formula of $C_{11}H_{12}N_4O_3S$ (M = 280.300). It decreased in peak area in HPLC diagrams as the reaction proceeded (data not shown). The m/z 297 $(M+17)^+$ signal corresponds to the intermediate arising from hydroxyl addition to the phenyl ring or pyrimidine ring of SMM, being formed through electron-transfer process by the effect of $SO_4^{\bullet-}$. $SMM^{\bullet+}$ is formed at first, and reacts quickly with H_2O by hydroxyl addition to generate hydroxyl addition product of (OH)SMM in an aqueous solution. The available information is yet not enough to determine which ring of SMM attacked by $SO_4^{\bullet-}$. The amino group activates aromatic ring toward an electrophilic substitution, so that probably the $SO_4^{\bullet-}$ attack occurs at the anilinic substructure. MS revealed another fragment of m/z 191. It is expected to be protonated hydroxyl sulfanilic acid, which originated from the cleavage of N-S bond of (OH)SMM and followed by hydroxyl addition reaction as discussed above. Another N–S bond cleavage induced compound was 4-methoxyl-2-aminopyrimidine. Its amino group (–NH_2) was oxidized to hydroxyl group (–OH) and hold characteristic fragments of m/z 126 because of the comparable oxidation potential of $SO_4^{\bullet-}$ to •OH. This is in accordance with the presence of phenol in aniline solution by the attack of •OH through more than one step [36].

Sulfonyl group can be evacuated by the attack of $SO_4^{\bullet-}$ at bonds of C–S and N–S, and extrusion of SO_2 proceeds on the basis of the common loss of 64 mass units. 4-Amino-N-(5-methoxy-3-pyrimidinyl)aniline, consisting of *p*-aminobenzene group linked to the pyrimidine ring through an NH bridge, with its protonated

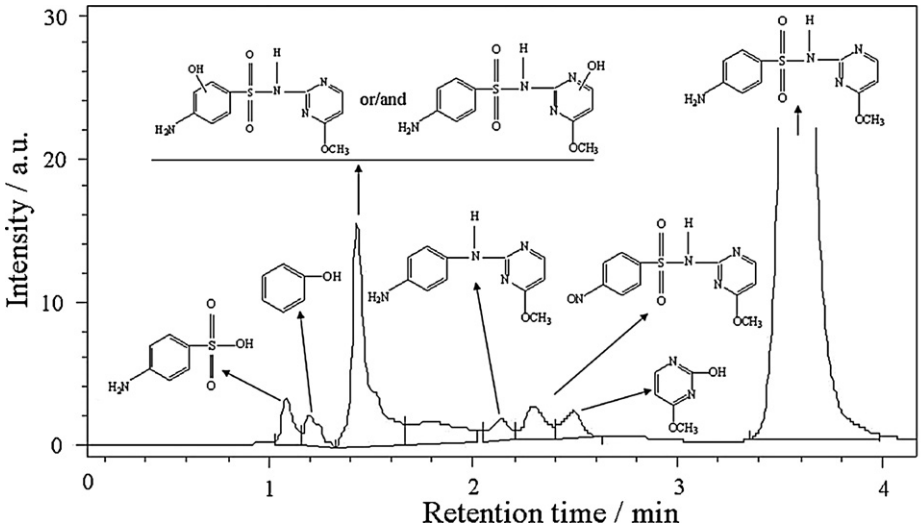

Fig. 6. LC–MS total ion chromatogram of SMM (c_0 = 0.06 mmol L^{-1}) obtained in the presence of 0.6 mmol L^{-1} $K_2S_2O_8$ and 1.2 mmol L^{-1} Fe_3O_4 MNPs after 10 min for reaction.

molecular ion peak of *m*/*z* 217 occurred in the MS spectra with retention time of 2.3 min. The phenomenon was frequently exhibited by sulfonamides in previous studies [32–34]. In addition to the SO_2 extrusion product, we have identified other oxidation products where the m/z is increased by 14 with *m*/*z* of 294 (M+14), which was identify as nitroso derivative, probably being generated by some redox pathways of primary amino group ($-NH_2$) on the aromatic ring. The same product was also detected by Guerad et al. [37] during the photodegradation of sulfadimethoxine.

The presence of fragment at *m*/*z* 94 in the MS spectrum with retention time of 1.2 min indicates the presence of phenol, which may originate from two pathways. In the first pathway, hydroxyl addition to SMM generates (OH)SMM with *m*/*z* of 297 at first, the cleavage of S–N bond of (OH)SMM occurred to form hydroxyl sulfanilic acid (*m*/*z* 191) and 4-methoxyl-2-aminopyrimidine subsequently. As H_2SO_4 extracted from the generated hydroxyl sulfanilic acid and its amino group was oxidized to hydroxyl group, phenol was formed in accordance with *m*/*z* 95. In the second pathway, the reaction of SO_2 extrusion happened initially to form 4-amino-N-(5-methoxy-3-pyrimidinyl)aniline. Aniline and 2-amino-4-methoxyl pyrimidine were generated by the cleavage of C–N at phenyl ring. Oxidation of amino group to hydroxyl group at aromatic ring and pyrimidine ring occurred successively to form phenol and 2-hydroxyl-4-methoxyl pyrimidine with *m*/*z* of 95 and *m*/*z* 126, respectively. The peak at *m*/*z* 213 in MS spectrum corresponding to the cleavage of two C–N bonds at pyrimidine ring of sulfamonomethoxine by high collision-induced dissociation. The same peak also appeared when using SMM standard. From the above-described results, the degradation pathway of SMM was list in Fig. 7.

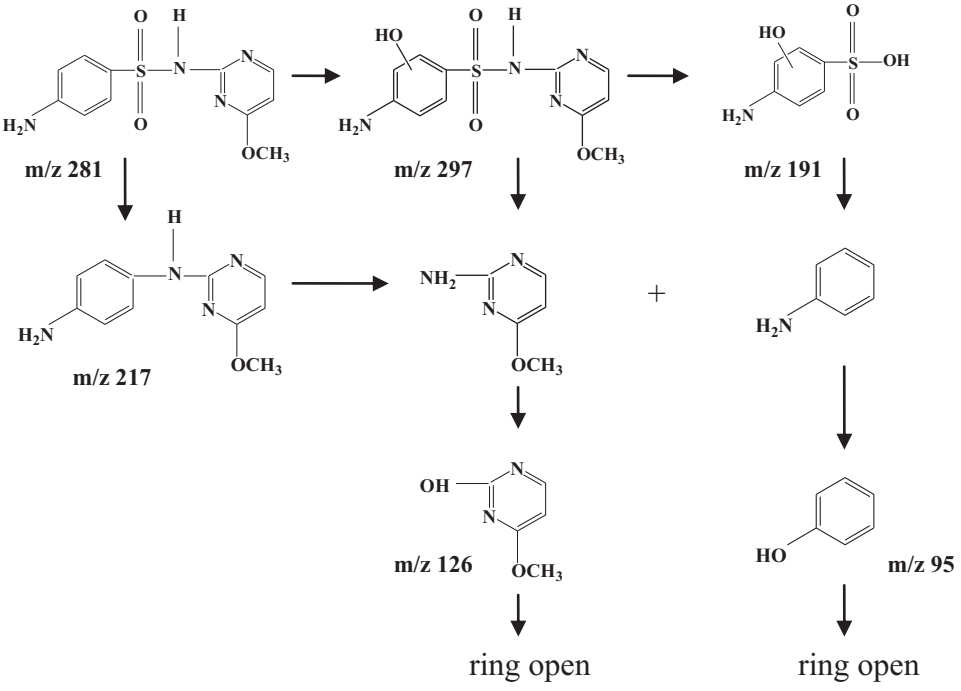

Fig. 7. Degradation pathways of SMM in $S_2O_8^{2-}$/Fe_3O_4 MNPs system.

4. Conclusions

An oxidative method was investigated for SMM degradation in heterogeneous activation system of Fe_3O_4 MNPs and persulfate. Reactive free radicals generated through Fe_3O_4 MNPs mediated activation of persulfate, leading to immediate degradation of SMM. In aqueous system, the effects of oxidant and Fe_3O_4 MNPs concentrations were studied for the $Fe_3O_4/S_2O_8^{2-}$ system and their molar ratio of Fe_3O_4 MNPs:$S_2O_8^{2-}$ was optimized at 2:1. The degradation removal of SMM was slightly dependent on solution pH values. When the initial solution pH was 7.0 or lower, the major free radicals were found to be $SO_4^{\bullet-}$, creating a very efficient degradation of SMM. When the initial solution pH was 8.5–10.0, the dominant free radicals are $SO_4^{\bullet-}$ and $^{\bullet}OH$, leading to a moderately effective degradation of SMM. In selected system of 2.40 mmol L^{-1} Fe_3O_4 MNPs and 1.20 mmol L^{-1} $K_2S_2O_8$, complete removal of SMM (c_0 = 0.06 mmol L^{-1}) was observed within 15 min. Based on the LC–MS analysis of the degradation intermediates, a full mechanism was proposed for the SMM degradation. This mechanism indicates that no potentially harmful intermediates generated and accumulated during the SMM degradation. Therefore, the activation of persulfate by Fe_3O_4 MNPs as a green oxidizing system has great potential applications in the degradation of organic toxic pollutants.

Acknowledgments

Financial supports from the National Science Foundation of China (Grants Nos. 20877031 and 21077037) and the National Science Foundation of Hubei Province (Grants No. 2009CDB078) are gratefully acknowledged. The Analytical and Testing Center of Huazhong University of Science and Technology is also thanked for its help in the characterization of the activator.

Appendix A. Supplementary data

Supplementary data associated with this article can be found, in the online version, at 10.1016/j.jhazmat.2010.12.017.

References

[1] N. Nakada, H. Shinohara, A. Murata, K. Kiri, S. Managaki, N. Sato, H. Takada, Removal of selected pharmaceuticals and personal care products (PPCPs) and endocrine-disrupting chemicals (EDCs) during sand filtration and ozonation at a municipal sewage treatment plant, Water Res. 41 (2007) 4373–4382.
[2] D.W. Kolpin, E.T. Furlong, M.T. Meyer, E.M. Thurman, S.D. Zaugg, L.B. Barber, H.T. Buxton, Pharmaceuticals, hormones, and other organic wastewater contaminants in U.S. streams, 1999–2000: a national reconnaissance, Environ. Sci. Technol. 36 (2002) 1202–1211.
[3] F. Lange, S. Cornelissen, D. Kubac, M.M. Sein, J.V. Sonntag, C.B. Hannich, A. Golloch, H.J. Heipieper, M. Möder, C.V. Sonntag, Degradation of macrolide antibiotics by ozone: a mechanistic case study with clarithromycin, Chemosphere 65 (2006) 17–23.
[4] M. Klavarioti, D. Mantzavinos, D. Kassinos, Removal of residual pharmaceuticals from aqueous systems by advanced oxidation processes, Environ. Int. 35 (2009) 402–417.
[5] F. Ingerslev, B. Halling-Sørensen, Biodegradability properties of sulphonamides in activated sludge, Environ. Toxicol. Chem. 19 (2000) 2467–2473.
[6] M. Stumpf, T.A. Ternes, R.D. Wilken, S.V. Rodrigues, W. Baumann, Polar drug residues in sewage and natural waters in the State of Rio de Janeiro, Brazil, Sci. Tot. Environ. 225 (1999) 135–141.
[7] N. Furusawa, Determining sulfamonomethoxine and its acetyl/hydroxyl metabolites in chicken plasma under organic solvent-free conditions, Anal. Bioanal. Chem. 385 (2006) 1570–1574.
[8] L.A. Poirier, D.R. Doerge, D.W. Gaylor, M.A. Miller, R.J. Lorentzen, D.A. Casciano, F.F. Kadlubar, B.A. Schwetz, An FDA review of sulfamethazine toxicity, Regul. Toxicol. Pharm. 30 (1999) 217–222.
[9] L. Lunar, D. Sicilia, S. Rubio, D. Pearez-Bendito, U. Nicke, Degradation of photographic developers by Fenton's reagent: condition optimization and kinetics for metal oxidation, Water Res. 34 (2000) 1791–1802.
[10] M. Panizza, G. Cerisola, Removal of pollutants from wastewater, Water Res. 35 (2001) 3987–3992.
[11] M.S. Lucas, J.A. Peres, Removal of COD from olive mill wastewater by Fenton's reagent: kinetic study, J. Hazard. Mater. 168 (2009) 1253–1259.
[12] C.J. Liang, Z.S. Wang, C.J. Bruell, Influence of pH in persulfate oxidation of TCE at ambient temperatures, Chemosphere 66 (2007) 106–113.
[13] C.J. Liang, C.J. Bruell, M.C. Marley, K.L. Sperry, Persulfate oxidation for in situ remediation of TCE. I. Activated by ferrous ion with and without a persulfate–thiosulfate redox couple, Chemosphere 55 (2004) 1213–1223.
[14] C.J. Liang, C.J. Bruell, M.C. Marley, K.L. Sperry, Persulfate oxidation for in situ remediation of TCE. II. Activated by chelated ferrous ion, Chemosphere 55 (2004) 1225–1233.
[15] C.J. Liang, C.F. Huang, Y.J. Chen, Potential for activated persulfate degradation of BTEX contamination, Water Res. 42 (2008) 4091–4100.
[16] A. Rastogi, S.R. Al-Abed, D.D. Dionysiou, Sulfate radical-based ferrous–peroxymonosulfate oxidative system for PCBs degradation in aqueous and sediment systems, Appl. Catal. B: Environ. 85 (2009) 171–179.
[17] S.Y. Oh, H.W. Kim, J.M. Park, H.S. Park, C. Yoon, Oxidation of polyvinyl alcohol by persulfate activated with heat, Fe^{2+}, and zero-valent iron, J. Hazard. Mater. 168 (2009) 346–351.
[18] Q.J. Yang, H. Choi, Y.J. Chen, D.D. Dionysiou, Heterogeneous activation of peroxymonosulfate by supported cobalt catalysts for the degradation of 2,4-dichlorophenol in water: the effect of support, cobalt precursor, and UV radiation, Appl. Catal. B: Environ. 77 (2008) 300–307.
[19] Q.J. Yang, H. Choi, S.R. Al-Abed, D.D. Dionysiou, Iron–cobalt mixed oxide nanocatalysts: heterogeneous peroxymonosulfate activation, cobalt leaching, and ferromagnetic properties for environmental applications, Appl. Catal. B: Environ. 88 (2009) 462–469.
[20] S. Vilhunen, M. Vilve, M. Vepsaelaeinen, M. Sillanpaeae, Removal of organic matter from a variety of water matrices by UV photolysis and UV/H_2O_2 method, J. Hazard. Mater. 179 (2010) 776–782.
[21] A. Zapata, S. Malato, J.A. Sanchez-Perez, I. Oller, M.I. Maldonado, Scale-up strategy for a combined solar photo-Fenton/biological system for remediation of pesticide-contaminated water, Catal. Today 151 (2010) 100–106.
[22] L. Gao, J. Zhuang, L. Nie, J. Zhang, Y. Zhang, N. Gu, T. Wang, J. Feng, D. Yang, S. Perrett, X. Yan, Intrinsic peroxidase-like activity of ferromagnetic nanoparticles, Nat. Nanotechnol. 2 (2007) 577–583.
[23] N. Wang, L. Zhu, M. Wang, D. Wang, H. Tang, Sono-enhanced degradation of dye pollutants with the use of H_2O_2 activated by Fe_3O_4 magnetic nanoparticles as peroxidase mimetic, Ultrason. Sonochem. 17 (2010) 78–83.
[24] N. Wang, L. Zhu, D. Wang, M. Wang, Z. Lin, H. Tang, Sono-assisted preparation of highly-efficient peroxidase-like Fe_3O_4 magnetic nanoparticles for catalytic removal of organic pollutants with H_2O_2, Ultrason. Sonochem. 17 (2010) 526–533.
[25] Q. Chang, K. Deng, L. Zhu, G. Jiang, C. Yu, H. Tang, Determination of hydrogen peroxide with the aid of peroxidase-like Fe_3O_4 magnetic nanoparticles as the catalyst, Microchim. Acta 165 (2009) 299–305.
[26] N.A. Frigerio, An iodometric method for the macro- and microdetermination of peroxydisulfate, Anal. Chem. 35 (1963) 412–413.
[27] H. Yan, J. Zhang, C. You, Z. Song, B. Yu, Y. Shen, Influences of different synthesis conditions on properties of Fe_3O_4 nanoparticles, Mater. Chem. Phys. 113 (2009) 46–52.
[28] G.V. Buxton, T.N. Malone, G.A. Salmon, Reaction of $SO_4^{\bullet-}$ with Fe^{2+}, Mn^{2+} and Cu^{2+} in aqueous solution, J. Chem. Soc., Faraday Trans. 93 (1997) 2893–2897.
[29] C.J. Liang, H.W. Su, Identification of sulfate and hydroxyl radicals in thermally activated persulfate, Ind. Eng. Chem. Res. 48 (2009) 5558–5562.
[30] M. Francesco, C. Attilio, Electron-transfer processes: peroxydisulfate, a useful and versatile reagent in organic chemistry, Acc. Chem. Res. 16 (1983) 27–32.
[31] M.N. Abellán, J. Giménez, S. Esplugas, Photocatalytic degradation of antibiotics: the case of sulfamethoxazole and trimethoprim, Catal. Today 144 (2009) 131–136.
[32] A. Boreen, W. Arnold, Kristophermcneill, Photochemical fate of sulfa drugs in the aquatic environment: sulfa drugs containing five-membered heterocyclic groups, Environ. Sci. Technol. 38 (2004) 3933–3940.
[33] A. Boreen, W. Arnold, Kristophermcneill, Triplet-sensitized photodegradation of sulfa drugs containing six-membered heterocyclic groups: identification of an SO_2 extrusion photoproduct, Environ. Sci. Technol. 39 (2005) 3630–3638.
[34] E. Vulliet, C. Emmelin, J.M. Chovelon, C. Guillard, J.M. Herrmann, Photocatalytic degradation of sulfonylurea herbicides in aqueous TiO_2, Appl. Catal. B: Environ. 38 (2002) 127–137.
[35] P. Calza, C. Medana, M. Pazzi, C. Baiocchi, E. Pelizzetti, Photocatalytic transformations of sulphonamides on titanium dioxide, Appl. Catal. B: Environ. 53 (2004) 63–69.
[36] J. Anotai, M.C. Lu, P. Chewpreecha, Kinetics of aniline degradation by Fenton and electro-Fenton processes, Water Res. 40 (2006) 184–1847.
[37] J.J. Guerad, Y.P. Chin, H. Mash, C.M. Hadad, Photochemical fate of sulfadimethoxine in aquaculture waters, Environ. Sci. Technol. 43 (2009) 8587–8592.